Electron Scavenging Study on the Photobleaching of Trapped Electrons in 3-Methylhexane Matrices at 77 K

Koichi OKA, Hideo YAMAZAKI, and Yoshihiko HATANO

Laboratory of Physical Chemistry, Tokyo Institute of Technology, Meguro-ku, Tokyo 152

(Received December 11, 1973)

The effect of addition of sulfur hexafluoride as an electron scavenger on quantum efficiency was investigated for the decay of trapped electrons in 3-methylhexane matrices at 77 K during photobleaching in the wavelength range 700—1900 nm. Since the quantum efficiency for the decay of trapped electrons in pure matrices is independent of the initial concentration, almost all the recombination of liberated electrons with the cations is geminate. The increase in quantum efficiency for the decay of trapped electrons by the addition of the electron scavenger SF_6 was analyzed quantitatively. The quantum efficiency for the photoliberation of trapped electrons from the trapping sites may be about unity. The liberated electrons in the absence of the electron scavenger are retrapped or neutralized. The ratio of the former process to the latter at a wavelength greater than 1500 nm is much larger than that at a shorter wavelength. The wavelength dependence of the ratios of the electron scavenging process to these processes has also been discussed.

The trapped electrons (e_t^-) produced by γ-irradiation in organic glasses at low temperature in the dark decay with infrared illumination (photobleaching)[1-4] or in the course of annealing (thermal bleaching).[5-7] The recombination-luminescence[8,9] and electric conductivity[10-12] have been measured during the course of bleaching. There are two states for electrons in glassy matrices, trapped electrons e_t^- and mobile electrons e_m^-, the former being stable and observable by optical absorption measurement or ESR, and the latter undergoing rapid retrapping or neutralization and not observable by the usual methods. Neutralization is either geminate or random. The decay of e_t^- might be due to either kind. The part of e_t^- geminately neutralized can not contribute to electric conductivity. The presence of electron scavengers suppresses the formation of e_t^-,[13] and increases the decay rate of e_t^- during the course of photobleaching.[1] More quantitative analysis of the photobleaching of e_t^- in 3-methylhexane glass (3MHX) and the effect of the addition of SF_6 as an electron scavenger have been carried out in order to estimate the quantum efficiency of the photoliberation of e_t^- from the trapping sites. The wavelength dependence of the fate of the photoliberated electrons has been examined in both the absence and presence of SF_6. The fate has been discussed in terms of the competition between the retrapping, neutralization and scavenging processes.

Experimental

3MHX (pure grade, Aldrich Chemical Co.) was purified by passing through an activated silica gel column. It was degassed by the freeze-pump method and trap-to-trap distillation, and stored on sodium-potassium alloy for more than a day before use. SF_6 (Matheson Co.) was used without purification.

In a mercury-free vacuum system, a constant volume (0.35 ml at room temperature) of 3 MHX was measured with a capillary of 2 mm diameter. The amounts of gaseous material added were determined by means of an oil manometer with a flask of a constant volume. The Ostwald absorption coefficient of SF_6 in liquid 3MHX at room temperature was about 1.3 and was used to determine the concentration of the solute in 3MHX glass at 77 K. The sample was sealed in a Suprasil quartz ESR tube (diameter 5 mm, volume 0.4 ml) and irradiated for 2.5—30 min with ^{60}Co γ-rays at 77 K in the dark at the dose rate (1.0—5.4) $\times 10^5$ r/hr. An aluminum foil was used to intercept the light emitted from Pyrex glass of a Dewar vessel during the course of γ-irradiation. After γ-irradiation, the ESR spectra of the samples were immediately measured in the dark with a JEP-1 X-band ESR spectrometer (JEOL) with field modulation 100 kHz. During repeated measurements by forward and backward scanning of the magnetic field, bleaching experiments were performed with monochromatic infrared light from a light source of QR-50 photospectrometer (Shimadzu). Actinometry was carried out with a photometer of thermocouple (JASCO) corrected by total light-intensity of a tungsten lamp (30 W; efficiency of the light emission 60%).

Results

The trapped electrons in γ-irradiated 3MHX matrices at 77 K were measured by ESR. The signal intensity of e_t^- decreased during the course of photo bleaching by infrared light, but not that of 3-methylhexyl radical. At a small microwave power of ESR, the saturation factor of the signal of e_t^- was almost constant during the course of photobleaching. The effect of photobleaching on the ESR signal intensity

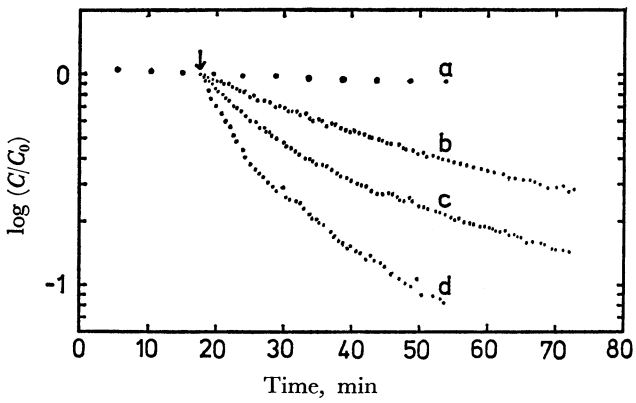

Fig. 1. The decay plots of log (C/C_0) against time in 3MHX after γ-irradiation: a) natural decay in the dark (dose $= 1.1 \times 10^{19}$ eV/g), and the decay due to photobleaching at $\lambda = 1500$ nm after elapse of the time indicated by arrow. The slit of the monochrometer was opened to various widths, namely b) 0.2, c) 0.3, d) 0.5 mm (dose $= 2.8 \times 10^{18}$ eV/g).

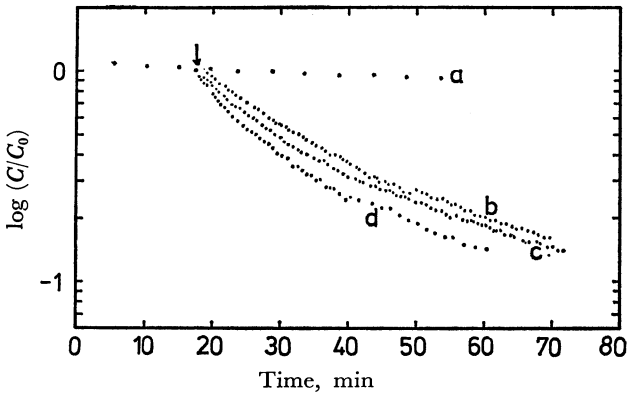

Fig. 2. The decay plots of log (C/C_0) against time after γ-irradiation: a) natural decay in the dark (γ-irradiation dose 1.1×10^{19} eV/g), and the decay due to photobleaching at $\lambda=1500$ nm with slit width 0.3 mm, in which the samples were γ-irradiated to various doses, namely b) 5.6, c) 2.8, d) 1.4 (10^{18} eV/g). The arrow on the curve indicates the starting point of infrared irradiation.

of e_t^- is given by C/C_0, the ratio of the concentration of e_t^- after and before photobleaching. Semilogarithmic plots of the decay of C/C_0 in the dark or under illumination of infrared light at $\lambda=1500$ nm are given in Fig. 1. The natural decay in the dark is negligibly small as compared with the decay due to photobleaching. At each slit width, the time necessary for C/C_0 to decay to the same value is roughly proportional to the light intensities which are proportional to the square of the slit width. At a fixed light intensity the decay rate decreased slightly with increasing doses of γ-irradiation (Fig. 2). This might be due to the nonuniformity of light intensity in a sample tube. The intensity of the light flux near the inlet of the light path is larger than that near the outlet because of the light absorption of e_t^-. Thus, the quantum efficiency for the decay of e_t^- during photobleaching Φ is given by[14]

$$-\frac{\mathrm{d}\log C}{\mathrm{d}t}=I\varepsilon\Phi\bar{Q} \qquad (1)$$

where I is light intensity, ε the extinction coefficient of e_t^- and $\bar{Q}$ the correction term attributed to the nonuniformity of light intensity in a sample tube. Assuming that the light flux is parallel in the cylindrical sample tube, $\bar{Q}$ is given as a function of D:

$$\bar{Q}=\frac{2}{\pi D\ln 10}\int_{-1}^{1}[1-\exp\{(-\ln 10)\,D\sqrt{1-y^2}\}]\mathrm{d}y \qquad (2)$$

where D $(=2\varepsilon CR)$ is the optical density of e_t^-, and R the radius of the cylinder. The value of $\bar{Q}$ approaches unity for a small value of D, namely for a small value of C or ε. The values $\varepsilon=3.0\times10^4$ l mol^{-1} cm^{-1} at 1700 nm, which is assumed to be equal to that in 3-methylpentane glass,[15] and $G(e_t^-)=0.9$,[16] are used for the calculation of Φ. An appropriate coefficient is necessary for the right term of Eq. 1.

If Φ is constant during the course of photobleaching, the plots of log (C/C_0) against time are nearly on a straight line. Actually, however, the slope or the value $(-\mathrm{d}\log C/\mathrm{d}t)$ decreases with increasing time

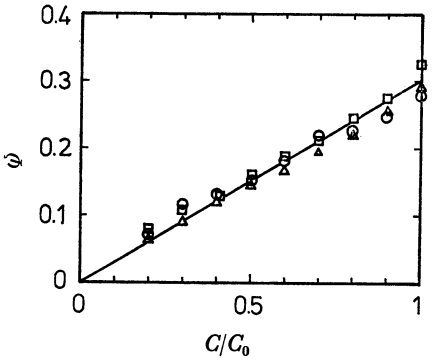

Fig. 3. Relation between Φ and C/C_0 at $\lambda=1500$ nm with slit width 0.3 mm in 3 MHX. Samples were γ-irradiated to various doses (10^{18} eV/g): ○ 1.4, △ 2.8, □ 5.6.

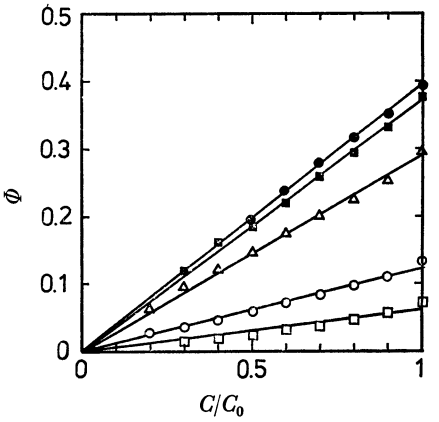

Fig. 4. Relation between Φ and C/C_0 at various wavelengths: ● 700, ■ 1300, △ 1500, ○ 1700, □ 1900 nm. This relation is also dose-independent as in Fig. 3.

(Fig. 1). The quantum efficiency for the decay of e_t^- calculated from the slopes by means of Eq. 1 decreases steadily with decreasing C/C_0. The values of Φ calculated from three series of measurements at different light intensities are almost the same for the same value of C/C_0. This shows that the main part of the primary act is a one-photon process.[17]

The efficiency Φ at 1500 nm is independent of γ-irradiation doses (Fig. 3). Also at $\lambda=1300$ nm, Φ is independent of γ-irradiation doses of $(0.28\text{—}5.7)\times10^{18}$ eV/g within 10% error. The dose-independence of γ-irradiation may support the validity of the correction term $\bar{Q}$. The relation between Φ and C/C_0 at various wavelengths is shown in Fig. 4. The plots are approximately on straight lines through origin, and represented approximately by

$$\Phi=\Phi_0(\lambda)C/C_0 \qquad (3)$$

where $\Phi_0(\lambda)$ is the initial quantum efficiency for the photobleaching at the wavelength λ, obtained from the value of Φ at $C/C_0=1$ (Fig. 4) and shown in Fig.9 as a function of the wavelength. The value of $\Phi_0(\lambda)$ is about 0.4 at 700—1300 nm. It decreases with increasing wavelength above 1300 nm. From Eqs.1 and 3 we obtain

$$-\frac{\mathrm{d}C/\mathrm{d}t}{C}=(\ln 10)I\varepsilon\bar{Q}\Phi_0\frac{C}{C_0} \qquad (4)$$

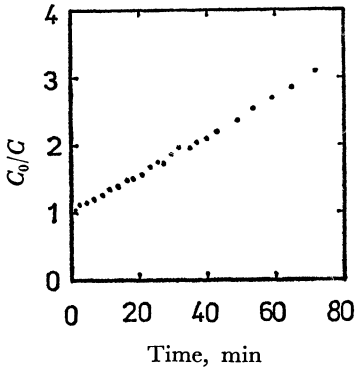

Fig. 5. Relation between C_0/C and time during photobleaching of e_t^- at $\lambda=700$ nm with slit width 1 mm (dose$=2.9\times10^{18}$ eV/g).

Since $\bar{Q}$ is regarded to be constant when either the concentration of e_t^- or the value ε is small, the solution of Eq. 4 is approximately given by

$$\frac{C_0}{C}=\Phi_0\left\{(\ln 10)I\varepsilon\bar{Q}t+\frac{1}{\Phi_0}\right\} \tag{5}$$

Substituting this into Eq. 3, we get

$$\Phi(t)=\left\{(\ln 10)I\varepsilon\bar{Q}t+\frac{1}{\Phi_0}\right\}^{-1} \tag{6}$$

The relation between C_0/C and time at wavelength 700 nm for small values of ε (Fig. 5) is in line with Eq. 5.

Since the time scale in the decay plots is influenced by both the light intensity and concentration of e_t^- (Figs. 1 and 2), we introduce a new variable T ($=\int(\ln 10)\,I\varepsilon\bar{Q}\,dt$). This is nearly proportional to t and experimentally approximated as

$$T=\sum_{j=1}^{n}(\ln 10)I\varepsilon\langle\bar{Q}\rangle_j\Delta t_j \tag{7}$$

where $C/C_0=1-j/10$ at t_j (j: integer), $\Delta t_j=t_j-t_{j-1}$, $\langle\bar{Q}\rangle_j$ is an average of $\bar{Q}$ between t_{j-1} and t_j. The exact solution of Eq. 4 is

$$\Phi(T)=\frac{1}{T+1/\Phi_0(\lambda)} \tag{8}$$

Thus the introduction of T gives a simple solution useful for the analysis of the results particularly in the presence of SF_6.

In the semilogarithmic decay plots (Fig. 6) of e_t^- in 3MHX containing SF_6, the γ-irradiation doses are controlled in order to obtain the same initial concentration of e_t^-. Although the natural decay of e_t^- in the dark is accelerated by the addition of SF_6, the slope is less than 5% of that of the photobleaching even at the highest concentration of SF_6. During photobleaching, the decay time at the same value of C/C_0 decreases with increasing concentration of SF_6, the decay curve becoming almost linear at high concentrations. Figure 7 shows Φ calculated from the slopes (Fig. 6) by means of Eq. 1. The efficiency is enhanced by the addition of SF_6. The decrement of Φ with decreasing C/C_0 is smaller in the presence than that in the absence of SF_6. At the same concentration of SF_6, Φ is smaller for high γ-irradiation

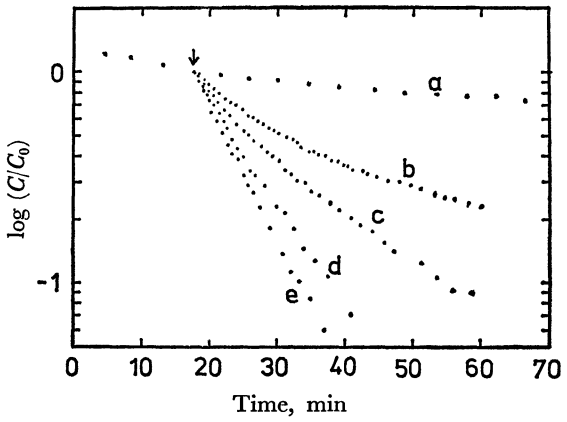

Fig. 6. The decay plots of log (C/C_0) against time in the dark and the decay due to photobleaching in the presence of SF_6 at $\lambda=900$ nm with slit width 0.7 mm: a) natural decay in the dark, $[SF_6]=9.7\times10^{-4}$ mol/l, irradiation dose$=5.6\times10^{18}$ eV/g, and the decay due to photobleaching, b) $[SF_6]=0$ mol/l, dose$=2.9\times10^{18}$ eV/g; c) $[SF_6]=1.7\times10^{-4}$ mol/l, dose$=2.1\times10^{18}$ eV/g; d) $[SF_6]=5.2\times10^{-4}$ mol/l, dose$=3.4\times10^{18}$ eV/g; e) $[SF_6]=9.7\times10^{-4}$ mol/l, dose$=7.7\times10^{18}$ eV/g. The initial concentrations of e_t^- (10^{-5} mol/l) are: a) 1.4; b) 3.8; c)d)e) 1.9. The arrow on the curve indicates the starting point of infrared irradiation.

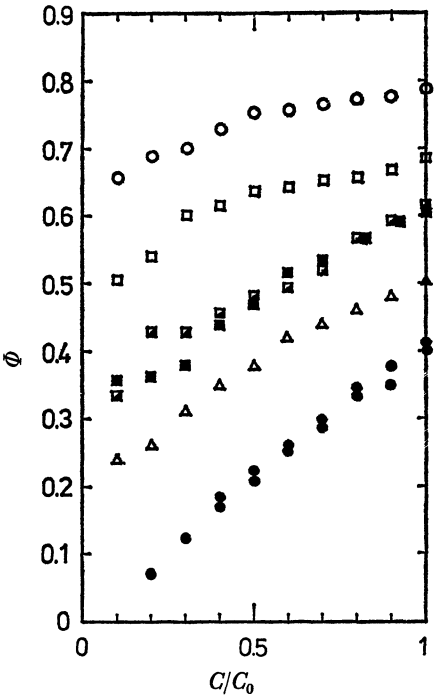

Fig. 7. Relation between Φ and C/C_0 in 3MHX γ-irradiated to various doses in the presence of various concentrations of SF_6 at $\lambda=900$ nm: ● $[SF_6]=0$ mol/l, dose$=2.9\times10^{18}$ eV/g; △ $[SF_6]=1.75\times10^{-4}$ mol/l, dose$=2.1\times10^{18}$ eV/g; □◪■ $[SF_6]=5.2\times10^{-4}$ mol/l, doses$=3.4$, 6.9, 21×10^{18} eV/g; ○ $[SF_6]=9.7\times10^{-4}$ mol/l, dose$=7.7\times10^{18}$ eV/g. The initial concentrations of e_t^- (10^{-5} mol/l) are: △□○ 1.9; ●◪ 3.8; ■ 12.

doses than that for the lower doses.

The effect of the addition of SF_6 on the relation between Φ and T is shown in Fig. 8. The samples were γ-irradiated in the two series of doses at various concentrations of SF_6. Efficiency Φ decreases gradually with increasing T calculated by means of Eq. 7. In pure matrices the plots almost fit the solid line given by Eq. 8. The initial concentration of e_t^- is 3.8×10^{-5} mol/l in the series of high γ-irradiation doses, and 1.9×10^{-5} mol/l in the series of low γ-irradiation doses. At each concentration of SF_6, Φ observed in the series of high irradiation doses is smaller than that of the low irradiation doses. The dose dependence of γ-irradiation in the presence of SF_6 (Figs. 7 and 8) suggests that SF_6 decomposes and produces less reactive molecules than SF_6 in electron scavenging reactions.

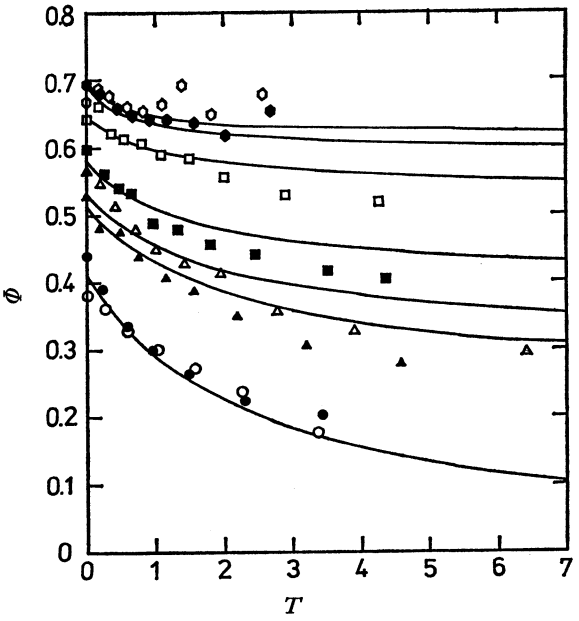

Fig. 8. Relation between Φ and T at $\lambda=1100$ nm in 3MHX containing various concentrations of SF_6 for various doses of γ-irradiation: ○● $[SF]_6=0$ mol/l, doses=1.4, 2.9×10^{18} eV/g; △▲ $[SF_6]=1.75\times10^{-4}$ mol/l, doses=2.3, 4.5×10^{18} eV/g; □■ $[SF_6]=5.2\times10^{-4}$ mol/l, doses=3.4, 6.9×10^{18} eV/g; ○● $[SF_6]=9.7\times10^{-4}$ mol/l, doses=7.7, 15.5×10^{18} eV/g. The initial concentration of e_t^- for the curves obtained by ○△□ and ○ is 1.9×10^{-5} mol/l, and for those by ●▲■ and ● 3.9×10^{-5} mol/l. The solid lines are the theoretical curves given by Eq. 13 when σ is 1, and b is selected to fit the experimental plots.

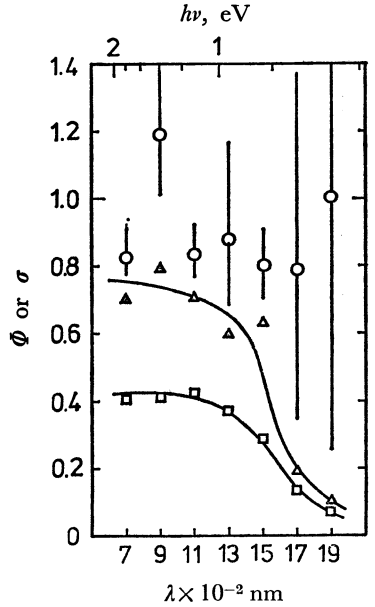

Fig. 9. Wavelength dependence of Φ or σ in the absence and presence of SF_6: □ Φ_0 in pure matrices, △ the initial value of Φ in the presence of SF_6 (9.7×10^{-4} mol/l); ○ σ obtained from the plots of Eq. 14.

The initial quantum efficiency for the decay of e_t^- is enhanced by the addition of SF_6 in the wavelength range 700—1900 nm (Fig. 9). At 700—900 nm, Φ becomes about 0.7 and can approach unity with increasing concentration of SF_6. At a wavelength greater than 1700 nm, the effect of the addition of SF_6 on the enhancement of Φ becomes less severe than that at shorter wavelength. It is difficult to know experimentally whether Φ approaches unity or not, since the ESR signal of e_t^- could not be observed at a high concentration of SF_6.

Discussion

The trapped electrons absorb the light in the infrared region and are liberated from the trapping sites in the following process.

$$e_t^- + h\nu \xrightarrow{\sigma} e_m^- \qquad (A)$$

where σ is the quantum efficiency of the primary photoliberation. Photo-liberated electrons or mobile electrons e_m^- move in matrices preceding neutralization with cations or preceding the retrapping into trapping sites (T.S.).

$$e_m^- + RH^+ \longrightarrow RH \qquad (B)$$

$$e_m^- + \text{T.S.} \xrightarrow{k_t} e_t^- \qquad (C)$$

Since the right term of Eq. 5 is independent of the initial concentration of e_t^-, the decay of e_t^- during photobleaching is a pseudo-second order process. The linear relation between C_0/C and time (Fig. 5) agrees with what is expected from Eq. 5. Since Φ_0 is not influenced by the change of initial concentration of e_t^-, the main part of the neutralization of e_t^- is geminate. The pseudo-second order processes depend probably on the probability distribution of the separation between e^-_t and cations. The main part of ion-pair separation should be smaller than the average ion-pair separation 230—600 Å, calculated from γ-irradiation doses assuming uniform distribution.

The relation between Φ and C, classified according to the type of neutralization, is given as a function of T in Table 1. The empirical relation of (2) represented by Eqs. 3 and 5 is applicable only to the non-polar hydrocarbon matrices.[1] Φ could be obtained as a function of C from the following factors characterizing the movement of electrons, *viz.*, the distribution of ion-pair separation, the range of Coulombic force of the parent cations and the mobility of e_m^-. The attractive force between electrons and cations pre-

Table 1. Φ as a function of C/C_0, and C as a function of T

Class number	Class of neutralization	$\Phi=-(dC/dT)/C$[a,b]	C/C_0[a,b]
1	geminate (strong attraction)	$\alpha(C/C_0)^{1/m}$; $m>1$	$(1+\alpha T/m)^{-m}$
2	geminate (intermediate attraction)	$\alpha C/C_0$	$(1+\alpha T)^{-1}$
3	geminate (weak attraction)	$\alpha C/C_0-\beta$; $C/C_0>\beta/\alpha$	$\left\{\frac{\alpha}{\beta}-\frac{\alpha-\beta}{\beta}\exp(-\beta T)\right\}^{-1}$
		0; $C/C_0<\beta/\alpha$	
4	random	αC	$(1+C_0\alpha T)^{-1}$

a) Classified according to the type of neutralization (see Appendix). b) α, β and m are constants.

scribed by the above factors might decrease in the order given. In (1) most of e_m^- is geminately neutralized and most of e_t^- can be easily photobleached. In (3), for a small concentration of ions, e_m^- escapes from a cation and cannot be neutralized randomly. In (4) random neutralization takes place because of uniform distribution of electrons and cations, the decay processes being of real-second order. The neutralization of e_m^- in a 2-methyltetrahydrofuran[3] glass is in an intermediate state between (3) and (4). (2) is distinguished from (4) by the role of C_0 in the equations. Experimentally the effect of γ-doses on Φ can differentiate the two types.

Diminution of Φ with the progress of photobleaching suggests that the neutralization process (B) decreases gradually as compared with the retrapping process (C). Since the rate of the geminate neutralization process is proportional to the probability density of e_m^- in the vicinity of the cations, and the position of e_t^- changes with repetition of photoliberation and reprapping, the gradual decrease of the role of recombination process may be caused by the gradual decrease of the probability density. A theoretical consideration is possible by means of prescribed diffusion approximation for an extended form[18] of the Smoluchowski equation.[19] In this approximation the rate of process (B) is given by KW, where K is a constant and W is the probability density of e_m^- in the vicinity of cations. The rate of process (C) is given by k_tS_t, where k_t is the rate constant and S_t is the concentration of the trapping sites. For the competition between (B) and (C), the quantum efficiency for the decay of e_t^- is given by

$$\Phi=\frac{\sigma KW(T)}{KW(T)+k_tS_t} \tag{9}$$

where $W(T)$ is a function of T, since the distribution of ion-pair separation changes with the progress of photobleaching. From Eqs. 8 and 9, we get

$$KW(T)=\frac{KW(0)}{(\sigma KW(0)/k_tS_t)T+1} \tag{10}$$

and

$$\frac{k_tS_t}{KW(0)}=\frac{\sigma}{\Phi_0}-1 \tag{11}$$

where k_t, K, σ, and Φ_0 are functions of λ.

In the presence of SF_6, the electron scavenging reaction competes with processes (B) and (C):

$$e_m^- + SF_6 \xrightarrow{k_s} SF_6^- \tag{D}$$

Since process (D) interrupts process (C), the value of Φ for a very large concentration of SF_6 might give the quantum efficiency σ. However, σ cannot be obtained by this method, since e_t^- is not formed at a very high concentration of SF_6. Efficiency Φ in the presence of SF_6 is given by

$$\Phi=\frac{\sigma(KW(T)+k_s[SF_6])}{KW(T)+k_tS_t+k_s[SF_6]} \tag{12}$$

Assuming that $KW(T)$ is given by Eq. 10 used in the case of pure 3MHX matrices, the following equations are obtained from Eqs. 10, 11 and 12:

$$\Phi(T)=\frac{(1-b/\sigma)^2}{T+1/\Phi_0-b/\sigma^2}+b \tag{13}$$

$$\frac{1}{b}=\frac{1}{\sigma}(1+k_tS_t/k_s[SF_6]) \tag{14}$$

The solid lines in Fig. 8 are given by Eq. 13 for the values of b selected to fit the plots at $\sigma=1$. Although the experimental data are scattered, the intercept of a straight line in plots of $1/b$ against $1/[SF_6]$ gives σ (Fig. 9). When σ is smaller than unity,

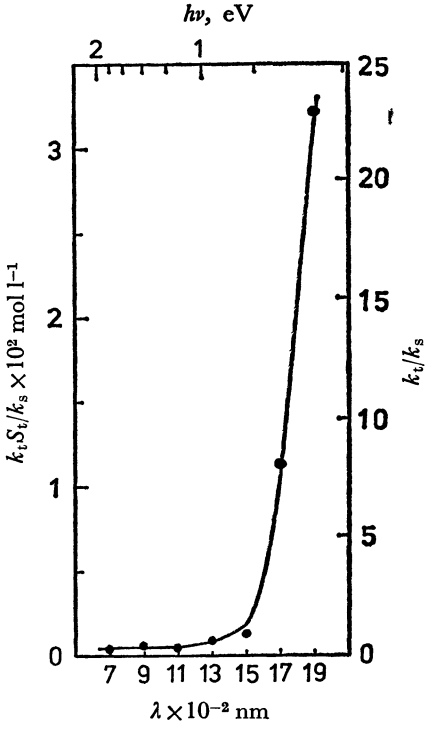

Fig. 10. Wavelength dependence of k_tS_t/k_s or k_t/k_s observed from the plots of Eq. 14 assuming that S_t is 1.4×10^{-3} mol/l.

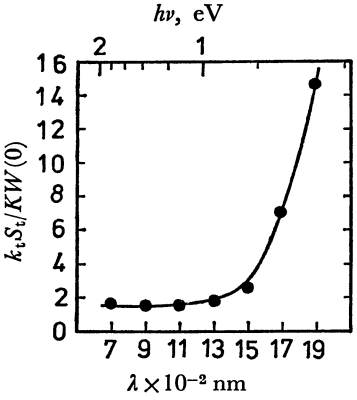

Fig. 11. Wavelength dependence of $k_tS_t/KW(0)$ estimated by means of Eq. 11.

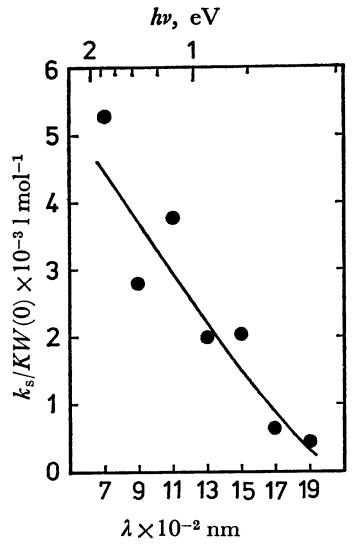

Fig. 12. Wavelength dependence $k_s/KW(0)$ calculated by means of Eq. 11 and the slope of the plots of Eq. 14.

Eq. 13 deviates from the plots to a greater extent than that at $\sigma=1$. Thus, σ might be about unity for wavelengths in the range 700—1900 nm.

Figure 10 shows the wavelength dependence of k_tS_t/k_s obtained from the slope of the straight line in the plots $1/b$ *vs.* $1/[SF_6]$. The minimum value of S_t is 1.4×10^{-3} mol/l which is estimated from the dose effect of γ-irradiation of the formation of e_t^-. The value of k_t/k_s is calculated by using this value of S_t. At a wavelength greater than 1500 nm, k_t/k_s becomes greater than that at a shorter wavelength. The value of $k_tS_t/KW(0)$ obtained from Eq. 11 becomes great at a wavelength greater than 1500 nm (Fig. 11). The value of $k_s/KW(0)$, calculated from the values of k_tS_t/k_s and $k_tS_t/KW(0)$, decreases gradually with increasing wavelength (Fig. 12). Because of a strong resemblance between Figs. 10 and 11, k_t increases markedly at a wavelength greater than 1500 nm. This wavelength dependence of k_t might show a relation between the translational energy of e_m^- and the track length of e_m^- from photoliberation to retrapping. The wavelength dependence of $k_s/KW(0)$ may be caused by the diffusion of e_m^- which separates electrons from cations.

The authors are gratefull to Professor Shoji Shida for his helpfull discussion.

Appendix

Calculation of Φ from the Decay Plot. During photobleaching, the concentration of e_t^-, C, decreases with time t. The rate of decay in a rectangular cell is given by

$$-\frac{dC}{dt}=\frac{I\Phi}{l}\{1-\exp(-\alpha lC)\} \tag{15}$$

where I is a light flux, $\alpha(=\varepsilon \ln 10)$ the extinction coefficient of e_t^-, Φ the quantum efficiency for the decay of e_t^- during photobleaching, and l the length of the cell. With the progress of photobleaching, the value of C at the inlet of light flux in the sample becomes smaller than that at the outlet, and the concentration becomes nonuniform. Equation 15 can be applied to this nonuniform sample by substituting the average concentration of e_t^- into C. The solution is found to be

$$\ln(\exp\alpha lC-1)=-I\int_{t_n}^{t}\Phi\alpha dt+\ln(\exp\alpha lC_n-1) \tag{16}$$

where C_n is the concentration of e_t^- at time t_n. Under conditions of a small αlC and a constant value of Φ, C is approximately given by exponential function:

$$C=C_n\exp\{-I\Phi\alpha(t-t_n)\} \tag{17}$$

For a large αlC, Eq. 16 is reduced to

$$C=-I\Phi(t-t_n)/l+C_n \tag{18}$$

At time t_n, Eq. 15 is given by

$$\left[\frac{d\ln C}{dt}\right]_{t_n}=-\frac{I\Phi\{1-\exp(-\alpha lC_n)\}}{lC_n} \tag{19}$$

which can be transformed into

$$\left[\frac{d\log C}{dt}\right]_{t_n}=-\varepsilon I\Phi Q \tag{20}$$

and

$$Q=\frac{1-\exp(-\alpha lC_n)}{\alpha lC_n} \tag{21}$$

In the case of a cylindrical tube, the parallel light flux is transmitted in the direction at right angle to the axis of the cylinder, and the length of light path is $l=2R\sqrt{1-y^2}$, where R is a radius of the cylinder. The effective Q is an averaged value such as

$$\bar{Q}=\int_{-1}^{1}Q\frac{2\sqrt{1-y^2}}{\pi}dy$$
$$=\frac{2}{\pi D\ln 10}\int_{-1}^{1}[1-\exp\{-D(\ln 10)\sqrt{1-y^2}\}]dy \tag{22}$$

where $D(=2\varepsilon C_nR)$ is the optical density of e_t^-.

Classification of the Geminate Reactions The experimental relation between Φ and C/C_0 can be classified as shown in Fig. 13. A speculative case given by curve (1) is expressed by

$$\Phi=\alpha(C/C_0)^{1/m},\quad m>1 \tag{23}$$

where the quantum efficiency of photobleaching is almost constant at the beginning of the photobleaching. Curve (1) corresponds to the photobleaching process of the trapped electrons, in narrow spatial distribution, in strong Coulombic field of parent ions and in weak diffusional movement. Curve (2) is given by

$$\Phi=\alpha(C/C_0) \tag{24}$$

The quantum efficiency of photobleaching is proportional to the value of C/C_0 as shown in Fig. 3. Curve (2) is observed

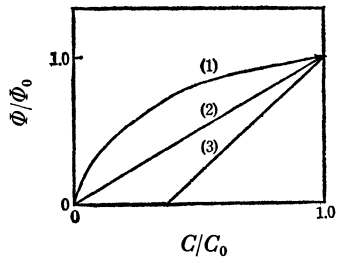

Fig. 13. Relation between Φ/Φ_0 and C/C_0 for the various types of geminate reaction: curve (1) strong attraction; curve (2) intermediate attraction; curve (3) weak attraction.

in the photobleaching process of the trapped electrons in nonpolar materices. Curve (3) can be written as

$$\Phi = \alpha(C/C_0) - \beta, \qquad C/C_0 > \beta/\alpha \qquad (25)$$
$$\Phi = 0, \qquad C/C_0 < \beta/\alpha$$

The quantum efficiency of photobleaching decreases with decreasing value of C/C_0 and becomes zero at a finite value of C/C_0. Therefore, as in the case of the neutralization in 2-methyltetrahydrofuran glass[3], it is difficult to observe a complete photobleaching. The functions in the last column of Table 1 can be obtained by integrating Eqs. 23—25.

References

1) D. W. Skelly, and W. H. Hamill, *J. Chem. Phys.*, **44**, 2891 (1966).
2) P. Hamlet and L. Kevan, *J. Amer. Chem. Soc.*, **93**, 1102 (1971).
3) P. J. Dyne and O. A. Miller, *Can. J. Chem.*, **43**, 2696 (1965).
4) H. B. Steen and J. Moan, *J. Phys. Chem.*, **76**, 3366 (1972).
5) J. B. Gallivan and W. H. Hamill, *J. Chem. Phys.*, **44**, 1279 (1966).
6) D. Soulter and J. E. Willard, *J. Phys. Chem.*, **76**, 3167 (1972).
7) F. S. Dainton, G. A. Salmon, and J. Teply, *Proc. Roy. Soc. Ser. A*, **286**, 27 (1965).
8) K. Funabashi, C. Herbert, and J. L. Magee, *J. Phys. Chem.*, **75**, 3221 (1971).
9) H. Yamazaki, K. Oka, M. Sato, and S. Shida, This Bulletin, **47**, 31 (1974).
10) L. Kevan, *J. Phys. Chem.*, **76**, 3830 (1972).
11) A. K. Munjal, and L. Kevan, *ibid.*, **76**, 2781 (1972).
12) B. Wiseal and J. E. Willard, *J. Chem. Phys.*, **46**, 4387 (1967).
13) a) T. Wakayama, T. Kimura, T. Miyazaki, K. Fueki, and Z. Kuri, This Bulletin, **42**, 266 (1969).
b) J. R. Miller, *J. Chem. Phys.*, **56**, 5173 (1972).
c) K. Oka, H. Yamazaki, and S. Shida, This Bulletin **46**, 2347 (1973).
14) Derivations are given in the Appendix.
15) W. H. Hamill, "Radical Ions," ed. by E. T. Kaiser and L. Kevan, Wiley-Interscience, New York, p. 353 (1968).
16) J. Lin, K. Tsuji, and F. Williams, *J. Amer. Chem. Soc.*, **90**, 2766 (1968).
17) A two photon process can occur to some extent in addition to the one photon process (Ref. 10).
18) A. Mozumder, *J. Chem. Phys.*, **55**, 3020 (1971).
19) M. V. Smoluchowski, *Ann. Phys.*, **48**, 1103 (1915).